

RAPIDLY-ROTATING LITHIUM-RICH K GIANTS: THE NEW CASE OF THE GIANT PDS 365

Natalia A. Drake^{1,2}, Ramiro de la Reza¹, Licio da Silva¹ & David L. Lambert³

¹*Observatório Nacional - Rio de Janeiro - Brazil*

²*Sobolev Astronomical Institute, St. Petersburg State University, Russia*

³*Department of Astronomy, University of Texas, USA*

drake@on.br

ABSTRACT

PDS 365 is a newly detected rapidly rotating ($v \sin i = 20 \text{ km s}^{-1}$) single low mass giant star which with HD 233517 and HD 219025 forms a remarkable ensemble of single K giants with the unique properties of rapid rotation, very strong Li lines, an asymmetrical $H\alpha$ profile, and a large far infrared excess. Their $v \sin i$ values are between 18 and 23 km s^{-1} , and LTE Li abundances, $\log \varepsilon(\text{Li})$, are between 2.9 and 3.9. Detailed analysis of PDS 365 reveals it to be a $\sim 1M_{\odot}$ giant with a value of $^{12}\text{C}/^{13}\text{C}$ approximately equal to 12. A clear relation between high rotational velocities and very high Li abundances for K giant stars is found only when asymmetrical $H\alpha$ profiles and large far-infrared excesses are present. If we consider single K giants, we find that among rapid ($v \sin i \geq 8 \text{ km s}^{-1}$) rotators, a very large proportion ($\sim 50\%$) are Li-rich giants. This proportion is in contrast with a very low proportion ($\sim 2\%$) of Li-rich stars among the much more common slowly rotating K giants. This striking difference is discussed in terms of proposed mechanisms for Li enrichment.

Subject headings: stars: abundances—stars: activity—stars: chemically peculiar—stars: circumstellar matter—stars: individual (PDS 365)—stars: mass loss—stars: rotation

1. INTRODUCTION

It is well known that single K giant stars are very slow rotators having a mean $v \sin i$ value of the order of 2 km s^{-1} (De Medeiros, Da Rocha & Mayor 1996). Rapidly rotating giants are rare; here, we consider a star with $v \sin i \geq 8 \text{ km s}^{-1}$ to be a rapid rotator. Currently, surveys with higher spectral resolution than previously used and new methods for measuring the $v \sin i$ values are uncovering additional examples of rapid rotators. One case is the giant HD 37434 with $v \sin i \simeq 65 \text{ km s}^{-1}$ (De Medeiros & Mayor 1999). Some previous searches of rapidly-rotating giants sought

to test and account for a possible relation between high chromospheric activity and the presence of strong Li lines. Some special surveys were then made in order to try to find correlations between rotation, chromospheric activity and Li abundance. Randich, Gratton, & Pallavicini (1993) and Randich, Giampapa, & Pallavicini (1994) did not find a correlation between rotation and Li for a group of chromospherically active giants. For a selected group of Li-rich K giants, De Medeiros, Melo, & Mayor (1996) found no correlation between Li and rotation.

De Medeiros et al. (2000) performed a statistical analysis to test the existence of a Li – rotation connection in single giants for stars hotter and cooler than G0 III, the spectral type marking the approximate boundary at which the average rotational velocity drops to the low values common among K giants. A general trend was found in that giants cooler than G0 III are characterized by lower rotation rates and lower Li abundances. It is the strong exceptions to this pattern that are the focus of our paper. For several years, the bright K1 III star HD 9746 was the only known rapidly rotating Li-rich giant ($v \sin i \sim 8 \text{ km s}^{-1}$). Now approximately twenty rapidly rotating K giants are known with varying levels of lithium abundance with several showing remarkable lithium overabundances relative to abundance expected and observed in the typical slowly rotating K giant for which the convective envelope has diluted the lithium abundance by a factor of about 50 relative to its main sequence value. In Table 1 we list all the apparently single K giants stars having $v \sin i \geq 8 \text{ km s}^{-1}$ together with their spectral types, Li abundances, and manifestations of activity. Comments on some individual stars are presented in the Appendix. These rapid rotators have been selected from the literature and have spectral types later than or equal to G8 (HD 6665 is an exception, see however the appendix notes on this star) and luminosity classes III, III/II and II. Unfortunately, a Li abundance remains to be obtained for some stars. The $v \sin i$ values were collected in general from three main sources (De Medeiros & Mayor 1999; Fekel & Balachandran 1993; Fekel 1997) in which rotation is measured by different techniques. In general, these works give similar values taking into account the errors involved. The only apparent exception is the extreme rotator HD 37434.

In considering HD 9746 and other rapidly rotating Li-rich giants, Fekel & Balachandran (1993) suggested a scenario to explain the relation between Li and rotation. The discovery that the majority of the Li-strong single giants present large far IR excesses (Gregório-Hetem et al. 1992; Gregório-Hetem, Castilho, & Barbuy 1993) introduced a new parameter – mass loss – into the discussion (de la Reza, Drake, & da Silva 1996). Following this, two interesting giants were discovered: HD 233517 (Fekel et al. 1996) and HD 219025 (Fekel & Watson 1998; Jasniewicz et al. 1999). Both are very Li-rich objects but are more rapidly rotating than HD 9746: the $v \sin i$ values of HD 233517 and HD 219025 are respectively 17.6 km s^{-1} (Balachandran et al. 2000) and 23 km s^{-1} (Jasniewicz et al. 1999), in contrast to 8.7 km s^{-1} for HD 9746.

In this paper, we present a new K giant star, PDS 365, with similar properties to HD 233517 and HD 219025. PDS 365 was discovered in the Pico dos Dias Survey (PDS) (Gregório-Hetem et al. 1992; Torres et al. 1995, Torres et al. 2002; de la Reza et al. 1997). In section 2, we present the main properties of this new object and in section 3, after inferring new properties of the rapidly

rotating single K giants, we discuss the problem of Li enrichment.

2. THE STAR PDS 365

2.1. Observations

The star PDS 365 classified as K1 III (Torres 1998, Torres et al. 2000) is a faint giant ($V = 13.15$ mag) and the optical counterpart of IRAS 13313 – 5838 with RAJ2000 and DECJ2000 equal respectively to $13^{\text{h}}34^{\text{m}}37.6^{\text{s}}$ and $-58^{\circ}53'34''$. It is located near the Galactic plane ($\ell = 308^{\circ}.5$, $b = 3^{\circ}.5$) and, in particular, near a complex of young stars found by Efremov & Sitnik (1988). The complex’s radial velocity relative to the LSR (-42 km s^{-1}) given by Efremov & Sitnik, is almost the same as the star’s velocity.

High dispersion spectra of the star PDS 365 were obtained in May 1996 with the 4.0 m telescope at CTIO, Chile, covering the wavelength interval between 5120 \AA and 8370 \AA at a spectral resolution of $R = 33,500$. Standard IRAF procedures were used for data reduction. Very high resolution spectra ($R = 181,000$) of the rapidly rotating stars HD 9746, HD 233517, and HD 203251 were obtained with the 2.7 m telescope of the McDonald Observatory. Nine spectra of HD 219025 and the spectra of HD 6665, HD 129989, HD 181475, HD 284857, ϵ Vir, and a second spectrum of PDS 365 were obtained with the 1.52 m telescope at La Silla, Chile, using the high resolution spectrograph FEROS under the Observatório Nacional (Brazil)/ESO agreement. The observation log is given in Table 2.

2.2. Fundamental Parameters

Our analysis of PDS 365 began by selecting as large a sample as possible of neutral and ionized iron lines free of blends. Line identifications and wavelengths were taken from Moore et al. (1966). After eliminating lines suspected to be blended, we used 21 Fe I and 3 Fe II lines for the determination of the fundamental stellar parameters. The oscillator strengths, $\log gf$, were taken from McWilliam & Rich (1994) who considered gf -values obtained by different authors and created a unique system by intercomparison of common $\log gf$ -values. Following the usual iterative procedure, we derived the effective temperature and microturbulence by requiring that the iron abundances be independent of excitation potential and of the equivalent width (EW) (Figure 1). The surface gravity, $\log g$, was derived from the ionization equilibrium equation by finding the value for which the iron abundances from Fe I and Fe II coincide. Table 3 lists the EW measurements, the $\log gf$ values, the low excitation potentials and final abundances. We derived the following parameters for PDS 365: $T_{\text{eff}} = 4540 \text{ K}$, $\log g = 2.2$, $\xi_{\text{m}} = 1.8 \text{ km s}^{-1}$ and $[\text{Fe}/\text{H}] = -0.09$. Line blending due to rapid rotation limits the number of unblended Fe II lines, and, hence, the accuracy of the $\log g$ determination. We estimate $\log g$ is accurate to about 0.3 dex. The synthetic spectrum

shown in Figure 2 calculated for the spectral region containing Fe II line 6084 Å suggests that our determination is a good one. Since the parallax of PDS 365 has not been measured, we adopt an absolute magnitude $M_V = 0.6$ mag, a typical value for K1 III stars (Schmidt-Kaler 1982). With this value, we estimate an approximate stellar luminosity, mass and radius: $L = 72M_\odot$, $M = 1.1M_\odot$ and $R = 14R_\odot$ respectively.

To calculate the distance to PDS 365 we used the photometric data obtained during the PDS (Torres et al. 2002): $V = 13.15$ and $(B - V)_{\text{obs}} = 1.50$. The typical value of color index for giants of this temperature is $(B - V)_0 = 1.10$ (Schmidt-Kaler 1982), which results in color excess of $E_{B-V} = 0.40$. Thus, the total absorption is $A_V = \mathfrak{R} \cdot E_{B-V} = 1.45$, where $\mathfrak{R} = 3.62$ was calculated using the formula from Schmidt-Kaler (1982). In this way, we derived a distance of PDS 365 of $d = 1.7$ kpc. The total absorption is contributed by the star’s circumstellar shell (CS) and the interstellar medium (IM): $A_V = A_V^{CS} + A_V^{IM}$. To separate the reddening due to the IM and CS and estimate an optical depth (τ_V) of the CS, we analyzed the well defined values of E_{B-V} of a sample of open clusters situated close to the line of sight to PDS 365. For the IM reddening, we used a value of $E_{B-V} = 0.25$ (Clariá 1980) determined for the open cluster NGC 5138 ($\ell = 307^\circ 55$, $b = +3^\circ 55$) which is situated at the distance of 1.8 kpc, almost the same as PDS 365. We thus estimated the absorption in the CS to be $A_V^{CS} = 0.55$ and $\tau_V = 0.50$. This inference of circumstellar extinction is qualitatively consistent with a far IR excess.

The projected rotational velocity ($v \sin i = 20 \text{ km s}^{-1}$) was obtained by means of a comparison of observed and synthetic spectra. Synthetic spectra were calculated with different values of $v \sin i$ with steps of 0.5 km s^{-1} . The precision of $v \sin i$ is of the order of 1 km s^{-1} . A macroturbulence velocity of 3 km s^{-1} was adopted as a typical value for red giants (Fekel 1997).

The radial velocity ($V_{\text{rad}} = -38.3 \pm 0.5 \text{ km s}^{-1}$) was obtained using telluric H₂O lines and O₂ lines as the comparison lines. H₂O wavelengths were taken from Lundström et al. (1991) and for O₂ from the catalog of Moore et al. (1966). Our recent FEROS spectrum of PDS 365 provided a new measurement of the radial velocity: $V_{\text{rad}} = -37.4 \pm 0.3 \text{ km s}^{-1}$ which agrees with the previous result. An old measurement using however a somewhat lower resolution, gave the value of $V_{\text{rad}} = -39 \text{ km s}^{-1}$ (Torres 1998). We conclude from these three measurements that PDS 365 appears to be a single star. Determined parameters of PDS 365 are summarized in Table 4.

2.3. Stellar Abundances

Using the fundamental parameters determined above, a detailed LTE spectral synthesis analysis was done using the current version of the MOOG program (Snedden 1973) and Kurucz (1993) atmospheric models to obtain CNO and Li abundances and the ¹²C/¹³C ratio. Due to the interdependence of C, N, and O abundances caused by the formation of molecules, an iterative scheme was implemented to derive the abundances of these elements. The head of the C₂ 0-1 band of the Swan $d^3\Pi_g - a^3\Pi_u$ system at 5635 Å was used in the determination of carbon abundance. The

wavelengths of C_2 ($^{12}C^{12}C$) molecular lines were taken from Phillips & Davis (1968). Electronic oscillator strength, $f_{el} = 0.33$, determined in Lambert (1978) was used in our calculations. Hönl-London factors were calculated using formulae from Kovacs (1969). The nitrogen abundance and the carbon isotope ratio $^{12}C/^{13}C$ were obtained by comparing the observed and theoretical line profiles for the ^{12}CN and ^{13}CN lines of 2-0 band of the CN red system $A^2\Pi - X^2\Sigma$ near 8000 Å. The wavelengths for ^{12}CN lines were taken from the list of Davis & Phillips (1963), and those for ^{13}CN from Wyller (1966). Oscillator strength of the band 2-0 of $f_{2-0} = 8.4 \times 10^{-4}$ determined by Sneden & Lambert (1982), due to extensive analysis of molecular lines belonging to different bands of CN red system, were used. The oscillator strengths of ^{13}CN lines were assumed to be those of the corresponding lines of ^{12}CN . The calculations were performed with the following dissociation potentials: $D(C_2) = 6.15$ eV, and $D(CN) = 7.65$ eV. The line lists were tested by fitting the solar and Arcturus spectra. The blending of C_2 0-1 lines and the Li I resonance line with faint CN lines was taken into account. Unfortunately, the presence of night sky emission at [O I] 6300 Å line prevented our use of this line to determine the oxygen abundance. This abundance was obtained indirectly by adopting the relation $[O/H] = 0.5[Fe/H]$ (Pagel & Tautvaišienė 1995) for stars with metallicity $[Fe/H] \geq -1.0$.

Results of the abundance analysis of PDS 365 are shown in Table 4 (where $C=^{12}C$). It would be interesting to compare the CNO abundances and $^{12}C/^{13}C$ ratio for PDS 365 with those corresponding of the other fast rotating Li-rich giants, but unfortunately they are generally not known. Three exceptions exist: HD 9746 with $^{12}C/^{13}C = 28 \pm 4$ (Brown et al. 1989), and $^{12}C/^{13}C = 24$ (Berdyugina & Savanov 1994), PDS 100, a high rotation Li-rich K giant, with $^{12}C/^{13}C = 9 \pm 1$ (Reddy et al. 2002) and the Li-poor giant, HD 112989 with a very low ratio $^{12}C/^{13}C = 3.4$ (Tomkin, Luck, & Lambert 1976). The low $^{12}C/^{13}C$ ratio found for PDS 365 of approximately equal to 12 (see Fig. 3) constitutes a strong indication that this star is indeed a giant star and not a young object. Other evidence showing that PDS 365 is not a young object is given by its $H\alpha$ absorption line. Its equivalent width of 1.4 Å is far larger than any EWs of the rare $H\alpha$ absorption lines found in pre-main-sequence objects which are mostly found in emission. Its $H\alpha$ equivalent width appears to be somewhat larger than the typical value of giants corresponding to 1.1 Å (Eaton 1995).

2.3.1. The CNO abundances

PDS 365 appears to present anomalous C and N abundances; they differ from those expected for a standard giant star that has already passed the first dredge-up convective phase in which ^{12}C is reduced and ^{14}N is increased by a larger factor than those inferred from Table 4. To confirm this behavior for PDS 365, we have determined by identical techniques the CNO abundances for a known standard Li-poor giant (ϵ Vir).

We chose ϵ Vir in part because it was analyzed by Kjærgaard et al. (1982) and they based the C abundance on the same C_2 5635 Å feature as used in this work for PDS 365. Our spectrum of ϵ Vir was obtained with FEROS. We have used similar values of T_{eff} , $\log g$, and microturbulence

to those used by Kjærgaard et al. (1982). The results are presented in Table 5 for which $[X/Fe]$ is the preferred indicator.

Our C abundance for ϵ Vir is larger by a factor of 0.10 dex than Kjærgaard et al.’s (1982). The main reason for this small difference is the treatment of weak blends on the blue side of the C_2 feature at 5635.195 Å. Kjærgaard et al. (1982) introduced weak neutral Fe lines with excitation potentials around 4.5 eV. We added C_2 molecular lines with high rotational quantum numbers from the data bank of Kurucz (1992).

However, the fact that our CNO abundances for ϵ Vir appear normal for a giant star highlights the apparently anomalous C and N abundances of PDS 365. In this respect, it is interesting to remark, as shown in Table 5, that similar C and N anomalies appear also to be present in PDS 100 and HD 9746 which are the only Li-rich rapidly-rotating giants with CNO values known in the literature. Curiously, Berdyugina & Savanov (1994) reported Li-rich, but slowly-rotating giants to have normal C and N abundances. Clearly, C, N, and O abundance studies should be extended to larger samples of Li-rich giants.

2.3.2. The Lithium abundances

In determining the Li abundance, we consider both the resonance 6708 Å line and the excited line at 6104 Å. In the spectral synthesis of the resonance Li line we used wavelengths and oscillator strengths from Andersen, Gustafsson & Lambert (1984), and for the secondary line we used the data from Lindgård & Nielsen (1977). For the former line, we considered the contribution of the isotope ^6Li in addition to the usual ^7Li . Three $^6\text{Li}/^7\text{Li}$ ratios equal to 0.0, 0.05, and 0.1 were taken into account and the resulting profiles calculated for the same total Li abundance equal to $\log \epsilon(\text{Li}) = 3.3$ are presented in Figure 4. For this Li abundance it is clear that the absence of ^6Li agrees better with observations. All attempts to fit the observations with a lesser Li abundance failed. In fact, for the case of $^6\text{Li}/^7\text{Li} = 0.1$ with an abundance of $\log \epsilon(\text{Li}) = 2.9$ we can fit the blue side and part of the center of the resonance line but the red wing will always be much too wide to fit this part of the line. Because the weak excited 6104 Å line is insensitive to the isotopic mix, we can conclude from our observations of the resonance line that ^6Li is absent. Figure 5 shows the synthetic (pure ^7Li) and observed spectra for the two lines. The same Li abundance, $\log \epsilon(\text{Li}) = 3.3$ fits both observed profiles.

Due to the star’s large rotational velocity, the blend at the blue side of the Li I line at 6104 Å is complex. We have been unable to match well the observed spectrum even using the most recent atomic data (VALD) on the blending Fe I and Ca I lines. In any case, the Li abundance obtained from this line, even with a small error due to this complex blend, is compatible with the Li abundance obtained from the resonance Li I at 6708 Å.

Non-LTE effects may affect the two Li lines differently. A first approximation to these effects can be estimated using calculations by Carlsson et al. (1994). For the effective temperature and

gravity of PDS 365, Carlsson et al.’s corrections are -0.17 for the resonance line and $+0.21$ for the secondary line. Nominally, this implies slightly different abundances from the two lines. Other non-LTE calculations include the effect of an overlying chromosphere (de la Reza & da Silva 1995), which may affect the sign and magnitude of the non-LTE calculations. It is clear, however, that the lithium enhancement of PDS 365 is only marginally affected by non-LTE effects.

2.4. Evidences of Chromospheric Activity and Mass Loss

PDS 365 has a large far-IR excess and a very asymmetrical $H\alpha$ profile. These properties are similar to those found in the three other rapidly rotating Li-rich giants discussed in this work. The $H\alpha$ line of PDS 365 and other rapidly rotating giants is shown in Fig. 6. The core of the line is blue-shifted relative to the rest frame of the star, and the blue wing is weakly in emission. One of the $H\alpha$ profiles of PDS 365 is very similar to that of HDE 233517 (Fig. 6). The core and wings of the $H\alpha$ profiles of these two stars resemble those of late-type supergiants (Mallik 1993; Eaton 1995) with chromospheric winds. Other phenomena indicative of even more energetic activity include the detection of X-rays and optical flares (Konstantinova-Antova & Antov 2000) from some of these stars (see Table 1). In this study, we consider a variable $H\alpha$ line as a manifestation of activity in these rapidly-rotating giants (see Fig. 6). The most striking case is that of HD 219025 with a variable central emission feature, and blue-shifted absorption in the core which varies even on a day-to-day basis (de la Reza et al. in preparation). These $H\alpha$ profiles may be produced by localized active regions on the stellar surface and modulated by rotation. The blue asymmetry is likely a signature of mass loss.

The signature of mass loss can be found in other spectral features (Na D lines) and in the far-IR excesses. Indeed, the Li-strong giants such as HD 233517 and HD 219025 present satellite absorption features in the blue wings of the resonance Na D lines. In a very high resolution spectrogram of HD 233517 obtained with the 2.7 m McDonald telescope, we detected several Na satellite lines; Balachandran et al. (2000) reported variations between the stellar and satellite lines. In the case of HD 219025, only one strong blue-shifted absorption was detected, but the variability of this absorption revealed by several spectra shows clearly that this line is not of interstellar origin.

Another way to investigate past mass loss episodes involves far-IR excesses measured by IRAS. Two color-color diagrams of IRAS fluxes are presented in Figures 7a and 7b for K giants in the IRAS catalog including the faint source extension. In Fig. 7a are plotted the rapid rotating K giants of Table 1. Fig. 7b which is similar to Fig. 1 of de la Reza et al. (1997) contains slowly rotating K giants. We must note, however, that for some stars rotational velocities remain to be measured. In both diagrams, three different regions labeled as I, II, and III are marked. Region I is defined by the photospheric colors, i.e., no far-IR excesses are present. The very large majority of Li-poor K giants belong to this region. Region II is the region where far IR excesses at 25 and 60 microns are pronounced. Region III is characterized by an excess at 60 microns. A scenario connecting a sudden ${}^7\text{Li}$ enrichment followed by an ejection of a detached CS and a subsequent ${}^7\text{Li}$

depletion has been proposed by de la Reza, Drake & da Silva (1996) and de la Reza et al. (1997) to explain the presence of K giants (rich or poor in Li) in these three regions. In this scenario, a complete CS ejection is represented by a loop beginning in region I, crossing regions II and III, and finishing again in region I.

Of the Li-rich ($\log \varepsilon(\text{Li}) \geq 1.5$) rapidly rotating stars, none falls in region I, the location of the vast majority of the slowly rotating and Li-poor giants. Considering the total of 18 rapidly rotating giants examined for lithium and plotted in Figure 7a, 4 of 18 are in region I but none are Li-rich. Three more of the 18 stars are in region II and each is extremely Li-rich. Region III hosts 11 stars with known Li abundances of which 6 are Li-rich. The Li-rich and very active single giant BD+70 959 (ET Dra) (Ambruster et al. 1997) has not been included in Fig. 7a because the association between the star and an IRAS source is uncertain. Stars HD 232862 and HD 185958 are also not represented in Fig. 7a. The first one, appears not to be an IRAS source and the second one has only upper limits of its fluxes at 25 and 60 microns and its corresponding point is out of the figure. For slowly rotating giants (Figure 7b), the vast majority are in region I with a very low percentage of Li-rich stars. For region II, 16 of 34 stars are Li-rich. There are 68 stars in region III of which 11 are Li-rich. Several stars lack a Li abundance determination. If these are excluded, the percentage of Li-rich stars increases slightly. Perhaps, the most noticeable statistics are the relative lack of rapidly rotating giants in region I, and the increased frequency of Li-rich rapidly rotating giants in regions II and III. Considering the 20 rapidly-rotating giants examined for Li in Table 1 (excluding BD+25 4819, possibly not a K giant, and HD 284857, not a rapid rotator), there are 10 Li-rich giants. This represents a very large ($\sim 50\%$) fraction of Li-rich giants if compared to the typical low proportion ($\sim 2\%$) (Brown et al. 1989) of Li-rich giants among the low rotators. These statistics encourage the speculation that the lithium enrichment is common among rapidly-rotating K giants.

In summary, we suggest four important (tentative) conclusions: 1) There is not a one to one relation between rotation and Li abundances. 2) Rapid rotation appears to be confined to spectral types between G8 and K2. This is probably a selection effect arising from the very large number of early type K giants in common catalogs. 3) An association of rapid rotation with a lithium enrichment appears when a high far IR excess is present. HD 9746 is an exception. 4) As noted above, Li enhancement is particularly common among rapidly rotating K giants but rare among slowly rotating giants. The first two conclusions have been found by other authors, but the last two are a new result of this work.

3. Lithium Enrichment of Giants

Single K giants are predominantly Li-poor, slowly rotating, and lacking a far IR excess. The baseline for lithium abundance in a K giant is set by the Li abundance that results from dilution arising from the giant’s convective envelope. This may be put at about $\log \varepsilon(\text{Li}) \leq 1.5$, a limit that allows for depletion of lithium by the main sequence progenitor as well as a deeper than predicted

convective envelope. Stars with a Li abundance in excess of this limit are declared to be Li-rich (see also Charbonnel & Balachandran 2000). Outstanding cases like PDS 365 are remarkably Li-rich with a Li abundance approaching or exceeding that expected of the star-forming cloud.

K giants that are rapidly rotating or Li-rich or having a far IR excesses are few in number. Often, the defining characteristics of these exceptional stars are correlated. When correlated, the implication must be that either a single process or related string of processes led to the anomalies. An imperfect correlation between excess rotation, lithium, and circumstellar material does not necessarily imply unrelated processes but rather may indicate different times and timescales for either the appearance or disappearance of the three exceptional observational characteristics.

These characteristics promote the following questions:

- Rapid rotation: Was this the result of the inhibition of the mechanism that reduces the surface angular rotation rate of most K giants? Or was angular momentum added to the envelope from the interior (e.g., a rapidly rotating core) or the exterior (e.g., a planet was swallowed)?
- Lithium: Was the lithium dilution experienced by normal K giants inhibited? Or was fresh lithium added to the envelope from the interior (e.g., ^3He was converted to ^7Li by the Cameron-Fowler [1971] mechanism), the surface (e.g., lithium production by stellar flares), the exterior (e.g., planets or brown dwarves were swallowed), or through a combination of interior, surface, and exterior processes?
- Far-infrared excess: Is the circumstellar material a residue of a protostellar disk/nebula or a dissolving planetary system? Or was the material ejected by the red giant or its immediate progenitor?

Presently, one scenario appears to account quite well for the existence in low numbers of rapidly rotating K giants, some of whom may be Li-rich and/or show a far IR excess. This is the idea that K giants may swallow a giant planet or brown dwarf. An idea, which in connection with lithium enrichment was first mooted by Alexander (1967), and was recently developed in some quantitative detail by Siess & Livio (1999a,b). Accretion and ingestion of giant planets or a brown dwarf by a red giant is shown by Siess & Livio (1999b) to account for a high Li abundance, a far IR excess, a rapid rotation, and X-ray emission in a few per cent of K giants, where the latter frequency is based in part on the observed frequency of low mass main sequence stars with planets.

In this scenario, the stellar lithium abundance saturates when the mass of accreted material approaches the mass of the convective envelope. Since the maximum abundance inferred for interstellar material and young main sequence stars is $\log \varepsilon(\text{Li}) \simeq 3.0 - 3.3$, one expects this to be the limit for stars that accrete interstellar-like material with an undepleted lithium abundance. This limit will not be reached, however, by accreting one or two giant planets; the Jovian mass is but one-thousandth of a solar mass. Accretion of 10 Jovian masses might raise the abundance to $\log \varepsilon(\text{Li}) \sim 1.5$ (Siess & Livio 1999b). Accretion of a brown dwarf with $M \sim 0.1M_{\odot}$ would put the

abundance close to the undepleted value, a value observed for PDS 365. Lithium abundances exceed the undepleted value in several cases; for example, Balachandran et al. (2000) obtain $\log \varepsilon(\text{Li}) = 4.2$ for HDE 233517. Accretion of terrestrial planets can, in principle, increase the lithium abundance above the initial/interstellar value but only if the mass of material from which those planets formed greatly exceeds the mass of the giant’s convective envelope. Alternatively, we note that Denissenkov & Weiss (2000, also Siess & Livio 1999b) propose that the accretion process triggers production of ${}^7\text{Li}$ from ${}^3\text{He}$ (see below) to provide additional lithium enrichment at the surface.

Charbonnel & Balachandran (2000) used Hipparcos parallaxes to place Li-rich giants on a Hertzsprung-Russell diagram, and to identify two favored luminosities for Li-rich stars. One sample including HD 9746, HDE 233517, and HD 219025 are at the ‘RGB bump’ where models show that the H-burning shell of low mass red giants burns through the molecular weight discontinuity left from the initial growth of the convective envelope that diluted the surface lithium and the ${}^{12}\text{C}/{}^{13}\text{C}$ ratio. (Intermediate mass Li-rich giants were found at a higher preferred luminosity associated with a molecular weight discontinuity predicted for the interior of an early-AGB star.) A trigger for Li-production was not suggested but the source of ${}^7\text{Li}$ was supposed to be ${}^3\text{He}$, a residue of the primordial ${}^3\text{He}$ and a product from partial operation of the pp -chain in the main sequence star.

Palacios, Charbonnel, & Forestini (2001) propose a trigger mechanism for the RGB-bump stars. Low mass stars at the luminosity of RGB bump burn ${}^3\text{He}$ to ${}^7\text{Be}$ (and then to ${}^4\text{He}$) just exterior to the H-burning shell but, as this is below the base of the convective envelope, the surface is not enriched in ${}^7\text{Li}$, the product of electron capture on ${}^7\text{Be}$. Palacios et al. invoke efficient diffusion of ${}^7\text{Be}$ into the region between the top of the H-burning shell and the base of the convective envelope. A consequence is a significant release of energy in this region primarily from ${}^7\text{Li}(p, \alpha)\alpha$ with the ${}^7\text{Li}$ formed from the ${}^7\text{Be}$. This Li-flash turns the region convective and it merges with the convective envelope enabling the surface ${}^7\text{Li}$ abundance to rise. Subsequent to the Li-flash, the surface Li is reduced because ${}^7\text{Li}$ is destroyed at the base of the convective envelope. Palacios et al. complete the connection between their theoretical account of Li-enrichment of red giants and the observations by two assumptions: (i) the required efficient diffusion is assumed related to rapid rotation of the core, and (ii) the luminosity increase from the Li-flash is assumed to result in mass-loss and formation of a dust shell.

Other proposals linking ${}^7\text{Li}$ to the reaction chain ${}^3\text{He}(\alpha, \gamma){}^7\text{Be}(e^-, \nu){}^7\text{Li}$ have been advanced but physical triggers for initiating the chain have not been identified (Fekel 1988; Fekel & Balachandran 1993; de la Reza, Drake, & da Silva 1996; de la Reza et al. 1997; Sackmann & Boothroyd 1999, 2000). In addition, the observational requirement for a coupling of lithium production to rotation and mass loss has been either overlooked or subject to nothing more than speculation.

Observations will likely decide whether the lithium of a Li-rich giant was synthesized internally or gathered by accretion. Differences in composition may be used to distinguish between the two hypotheses. Accretion or ingestion increases not only the lithium abundance but also the Be and B abundances, two light elements whose abundances were also reduced by the giant’s convective

envelope. Castilho et al. (1999) found Be underabundant in two Li-rich giants (HD 787 and HD 146850) and concluded that lithium had been produced internally. Neither giant is a rapid rotator. Comparisons of the C, N, and O isotopic and elemental abundances for Li-rich giants with those of normal giants are likely to prove instructive.

An obvious additional test involves the lithium isotopic ratio. Internal production implies the surface lithium should be pure ${}^7\text{Li}$. Ingestion of a giant planet adds ${}^7\text{Li}$ and ${}^6\text{Li}$ with an abundance ratio presumably equal to that of the star’s natal interstellar cloud. One supposes that this ratio is similar to the meteoritic ratio (${}^7\text{Li}/{}^6\text{Li} = 12$) and the local interstellar ratio, which is generally similar to the meteoritic ratio but one gross exception is known (Knauth et al. 2000). Our analysis of the 6707 Å feature in PDS 365 showed ${}^6\text{Li}$ to be absent. While positive detection of ${}^6\text{Li}$ would certainly have supported the hypothesis of ingestion, the failure to detect ${}^6\text{Li}$ does not necessarily require rejection of the hypothesis because even mild internal destruction of lithium following ingestion will lead to very severe losses of ${}^6\text{Li}$ because its destruction by protons occurs 70 times faster than the destruction of ${}^7\text{Li}$. Additionally, if ingestion serves as a trigger for ${}^7\text{Li}$ production from ${}^3\text{He}$, the ${}^6\text{Li}$ abundance may remain low and even undetectable.

Three other Li-rich giants fail to show ${}^6\text{Li}$. Reddy et al. (2002) from 6707 Å line profile analysis for a giant (PDS 100) with $\log \varepsilon(\text{Li}) = 2.5$ found no ${}^6\text{Li}$. Balachandran et al. (2000) excluded the presence of ${}^6\text{Li}$ at (or above) the meteoritic abundance in the Li-rich giants HD 9746 and HDE 233517 not from line profile analysis but on the grounds that the abundance derived from the very strong 6707 Å resonance doublet and the weaker 6103 Å secondary line were greatly different when ${}^6\text{Li}$ was included in the analysis. With an isotopic shift of 0.15 Å, the presence of ${}^6\text{Li}$ reduces the abundance needed to fit the equivalent width of the saturated 6707 Å line. Applied in this way, the test for ${}^6\text{Li}$ is not definitive because there are other ways to change the equivalent width of strong lines: e.g., modification of the microturbulent velocity field assumed to be isotropic and depth independent, changes to the outer layers of the model atmosphere, alternative model atmospheres, non-LTE effects. A new attempt to measure the ${}^6\text{Li}$ concentration should be made, with a much higher resolution, as used in this work, using the profile of the Li I 6707 Å line along with a parallel analysis of other strong lines of atom of low ionization potential, e.g., the Na D lines, the K I 7699 Å line and possibly the Ca I lines. Although the initial searches for ${}^6\text{Li}$ have been unsuccessful, a single detection would be an enormous stimulant to the search for the mechanism responsible for lithium enrichment of these red giants.

4. Conclusions

In this paper, we report on the discovery of a new rapidly rotating Li-rich K giant PDS 365, and discuss some general properties of an ensemble of high rotating K giants with $v \sin i \geq 8 \text{ km s}^{-1}$. There is a correlation between rapid rotation, mass loss as measured by the far IR excesses and an asymmetric $\text{H}\alpha$ line, and a high Li abundance. At present, one theoretical explanation explains in broad terms these connections: ingestion of material by the red giant provides lithium enrichment,

increases the angular momentum of the giant’s envelope, and stimulates mass loss. Additional lithium enrichment may occur because the accreted material in penetrating deep into the convective envelope to just above the hydrogen burning shell may trigger conversion of ^3He to ^7Li .

Red giants harbor an adequate supply of ^3He from which to synthesize ^7Li by the Cameron-Fowler mechanism. Palacios et al. (2001) have suggested that the Li-flash may operate in giants at the RGB bump, and speculated on a connection between the efficacy of the flash and rotation. This scenario not only agrees with the sudden ^7Li -enrichment – mass loss connection proposed by de la Reza et al. (1996, 1997) but, also, supports and enhances the necessity of considering stellar rotation in understanding the Li phenomena and this is the main subject of this paper. Observational tests involving the determination of the ^6Li , Be, and B abundances should serve to distinguish stars that gained lithium by ingestion from those that synthesized it internally.

Nature is so rich in phenomena that one should not insist that all Li-rich giants be traceable to a single origin. Three origins presently compete for observational approval: ingestion of material (brown dwarf, giant planets, and terrestrial planets), ingestion followed by triggered production of ^7Li from the stellar reservoir of ^3He , and internal activation of the ^3He reservoir. PDS 365 would appear to have a lithium abundance in excess of that directly obtainable by ingestion.

N.A.D. thanks FAPERJ for the financial support under the grants E-26/151.172/98 and E-26/171.647/99 and L. da S. thanks the CNPq for grant 200580/97-0. DLL acknowledges the support of the Robert A. Welch Foundation of Houston, Texas. We thanks the referee for important suggestions that improved the presentation of this paper. SIMBAD and VALD services have been used in this work.

A. Comments on some individual stars.

BD+25 4819. We have recently observed this star spectroscopically. Its spectrum appears to correspond to a star hotter than K0 II, the spectral type given in the literature. Its H α EW, equal to 3.2 Å is much larger than a typical EW of a G5 - M5 giant of 1.1 Å (Eaton 1995). Li lines are undetectable.

BD+31 2471. No studies of this star in the Li spectral region are known in the literature.

HD 6665. This Li-rich giant was found by Strassmeier et al. (2000) who give a projected rotational velocity $v \sin i = 10.0 \text{ km s}^{-1}$ and 7.9 km s^{-1} . We found a lower value of $v \sin i = 6.0 \text{ km s}^{-1}$ which includes the macroturbulent velocity. Using the stellar temperature $T_{\text{eff}} = 4500 \text{ K}$ given by Strassmeier et al. (2000) and adopting $\log g = 2.00$ and $[\text{Fe}/\text{H}] = 0.0$ we obtain a LTE Li abundance of $\log \varepsilon(\text{Li}) = 2.7$. A detailed analysis of this star will be presented later. Strassmeier et al. (2000) considered this star as G5 III nevertheless, a later type would be more consistent with its observed $B - V$ value of 1.19. However, the $B - V$ value of this star, used for the T_{eff} determination, may be affected by the absorption of a circumstellar shell. The use of a somewhat higher temperature will enhance the Li abundance.

HD 9746 = OP And is a well-known Li-rich giant discovered by Brown et al. (1989) that has been studied by several authors. This star has rather high C/N ratio equal to 3.89 (Berdyugina & Savanov 1994) and $^{12}\text{C}/^{13}\text{C} = 28 \pm 4$ (Brown et al. 1989). For stellar parameters proposed by Brown et al. (1989) ($T_{\text{eff}}, \log g, [\text{Fe}/\text{H}]$) equal to (4420, 2.3, -0.13) which are similar to those used by Pavlenko et al. (1999) and Balachandran et al. (2000), we derived an LTE Li abundance value $\log \varepsilon(\text{Li}) = 3.5$ using both resonance and subordinate Li lines, which is in good agreement with the value $\log \varepsilon(\text{Li}) = 3.6$ obtained by Pavlenko et al. (1999) with allowance for non-LTE effects. A photometric period of 76 days has been proposed by Strassmeier & Hall (1988). We note the high level of activity as indicated by very strong single-peaked Ca II H and K emission lines (Smith & Shetrone 2000) and X-ray emission. This star was found to flare by Konstantinova-Antova & Antov (2000).

HD 31993. Three spectra of this star obtained on successive nights show variations of the H α line's EW (1.56 Å, 1.24 Å, and 1.18 Å). The photometric period is 28 days (Hooten & Hall 1990, Strassmeier et al. 1997).

HD 33798. This low mass star ($M = 1.8M_{\odot}$, Gondoin 1999) was studied by Fekel & Marshall (1991). They found no periodic radial velocity variation and suggested that the star is single. Magnitude variations with the period of $P = 9.825$ days were found (Hooten & Hall 1990), which with $v \sin i = 29 \text{ km s}^{-1}$ measured by Fekel & Marshall (1991) results in $R \sin i = (5.6 \pm 0.4)R_{\odot}$. The Hipparcos parallax of $\pi = 8.94 \pm 1.35 \text{ mas}$ results in $M_V = 1.68$, $R = 6.7R_{\odot}$, $i = 57^{\circ}$, and an equatorial rotation velocity $v_{\text{eq}} = 35 \text{ km s}^{-1}$. Gondoin (1999), due to its high X-ray luminosity ($L_X = 1074.7 \cdot 10^{27} \text{ erg s}^{-1}$), considers this star to be a FK Comae candidate. Hipparcos observations revealed a faint companion star with angular separation of $0.358 \pm 0.011 \text{ arcsec}$, and

$\Delta V = 1.85 \pm 0.08$ mag. Flare activity on this star have been detected by Konstantinova-Antova, Antov, & Bachev (2000).

HD 39152. No information on the Li spectral region has been found in the literature.

HD 68776. Small-amplitude variable star ($\Delta V = 0.145$ mag, Percy et al. 1994). Adopting the stellar parameters (T_{eff} , $\log g$, $[\text{Fe}/\text{H}]$) equal to (4750, 2.5, 0.00) we derived an LTE Li abundance value of $\log \varepsilon(\text{Li}) = 1.1$. This star has a symmetrical $\text{H}\alpha$ profile with an EW equal to 1.26 Å. Ca II emission is absent.

HD 112989 = 37 Com. This intermediate mass star ($M = 5.0M_{\odot}$, De Medeiros et al. 1999) has the very low ratio $^{12}\text{C}/^{13}\text{C}=3.4$, equal to the CN-cycle’s equilibrium value (Tomkin et al. 1976). The low carbon/nitrogen ratio $\text{C}/\text{N}=0.8$ (Lambert & Ries 1981) also points to a strong mixing undergone by this star. De Medeiros et al. (1999) found significant Ca II H and K emission variability. Henry et al. (2000) found a periodicity of $P = 70$ days, and $i = 17^{\circ}$ and noted that the star may undergo radial pulsations.

HD 129989. Moderate X-ray luminosity $L_X \leq 5.1 \cdot 10^{28}$ erg s $^{-1}$, intermediate mass, $M = 4.6M_{\odot}$, star (Gondoin 1999). A recent high resolution spectrum of this star obtained in this work shows the Li line to be absent.

HD 145001. A high X-ray luminosity ($L_X = 3.318 \cdot 10^{30}$ erg s $^{-1}$) intermediate mass star ($M = 3.4M_{\odot}$, Gondoin 1999)

HD 181475. Henry, Fekel, & Hall (1995) found a variability of $\Delta V = 0.06$ mag with a periodicity of $P = 31 \pm 1$ days and presumed that this is due to pulsations. Hipparcos data confirmed this variability giving an intrinsic variability amplitude of 0.055 ± 0.013 mag. A recent spectrum of this star obtained in this work presents no Li lines.

HD 185958. CN-strong star ($\text{C}/\text{O}=0.50$, Mishenina & Tsymbal 1997).

HD 199098. No studies are known of this star in the Li spectral region.

HD 203251. For this rapid rotator we found LTE Li abundance equal to $\log \varepsilon(\text{Li}) = 1.5$ similar to that presented by Fekel & Balachandran (1993) (1.4) using the following stellar parameters (T_{eff} , $\log g$, $[\text{Fe}/\text{H}]$) equal to (4500, 3.00, -0.3).

HD 219025. Even if Houk & Cowley (1975) classified this star as K2 IIIp, other authors, as Whitelock et al. (1995) and Randich et al. (1993) suggested that this star could be a pre-main sequence star. Also a RS CVn-type class was proposed for this star by Cutispoto (1995). Fekel et al. (1996) gave convincing arguments indicating that this star is in reality a giant star with a radius of $18.2R_{\odot}$. Our large number of spectra obtained for this star (see Table 2) do not show the presence of duplicity. A rotational velocity of 23 ± 3 km s $^{-1}$ was measured by Jasiewicz et al. (1999). With stellar parameters, similar to those proposed by Jasiewicz et al. (T_{eff} , $\log g$, $[\text{Fe}/\text{H}]$) equal to (4500, 2.0, -0.1) we deduce a Li abundance of $\log \varepsilon(\text{Li}) = 2.9$. Fekel & Watson (1998) obtained a larger LTE Li abundance of 3.3 using a hotter atmosphere ($T_{\text{eff}} = 4640$ K) and a larger

Li EW. As mentioned in section 2.4 due to its interesting properties of variability this star will be the subject of a subsequent separate work (de la Reza et al. in preparation).

HD 232862. No information on the Li spectral region has been found in the literature.

HD 233517. This star has been considered in the recent past a main sequence Vega-type star (Skinner et al. 1995). However, Fekel et al. (1996) showed that this star is not only a single giant but also a very Li-rich star. Drake (1998) found a LTE Li abundance of $\log \varepsilon(\text{Li}) = 3.9$ using the following stellar parameters (T_{eff} , $\log g$, $[\text{Fe}/\text{H}]$) equal to (4470, 1.42, -0.45), similar, except the gravity, to those proposed by Balachandran et al. (2000).

HD 284857. This is a relatively unknown star in the literature. We calculated a Li abundance of $\log \varepsilon(\text{Li}) \simeq 0.3$ adopting the following stellar parameters: (T_{eff} , $\log g$, $[\text{Fe}/\text{H}]$) equal to (4250, 1.5, 0.00) In any case, this giant cannot be considered a rapidly-rotating star. Our measured $v \sin i$ value is only 4.5 km s^{-1} . The equivalent width of the symmetrical $\text{H}\alpha$ line is 1.4 \AA .

REFERENCES

- Alexander, J.B. 1967, *The Observatory*, 87, 238
- Ambruster, C. W., Fekel, F.C., Guinan, E.F., & Hrivnak, B. J. 1997, *ApJ*, 479, 960
- Andersen, J., Gustafsson, B., & Lambert, D.L. 1984, *A&A*, 136, 65
- Balachandran, S.C., Fekel, F.C., Henry, G.W., & Uitenbroek, H. 2000, *ApJ*, 542, 978
- Berdyugina, S.V., & Savanov, I.S. 1994, *Astron. Letters*, 20, 639
- Brown, J.A., Sneden, C., Lambert, D.L., & Dutchover, E. 1989, *ApJS*, 71, 293
- Cameron, A.G.W., & Fowler, W.A. 1971, *ApJ*, 164, 111
- Carlsson, M., Rutten, R.J., Bruls, J.H.M.J., & Shchukina, N.G. 1994, *A&A*, 288, 860
- Castilho, B. V., Spite, F., Barbuy, B., Spite, M., de Medeiros, J. R., & Gregorio-Hetem, J. 1999, *A&A*, 345, 249
- Castilho, B. V., Gregorio-Hetem, J., Spite, F., Barbuy, B., & Spite, M. 2000, *A&A*, 364, 674
- Charbonnel, C., & Balachandran, S.C. 2000, *A&A*, 359, 563
- Clariá, J.J. 1980, *Ap&SS*, 72, 347
- Cutispoto, G. 1995, *A&AS*, 111, 507
- Davis, S.P., & Phillips, J.G. 1963, *The Red System ($A^2\Pi - X^2\Sigma$) of the CN Molecule*, University of California Press, Berkley and Los Angeles

- de la Reza, R., & da Silva, L. 1995, *ApJ*, 439, 917
- de la Reza, R., Drake, N.A., & da Silva, L. 1996, *ApJ*, 456, L115
- de la Reza, R., Drake, N.A., da Silva, L., Torres, C.A.O., & Martin, E.L. 1997, *ApJ*, 482, L77
- De Medeiros, J.R., Melo, C.H.F., & Mayor, M. 1996, *A&A*, 309, 465
- De Medeiros, J.R., Da Rocha, C., & Mayor, M. 1996, *A&A*, 314, 499
- De Medeiros, J.R., & Mayor, M. 1999, *A&AS*, 139, 433
- De Medeiros, J.R., Konstantinova-Antova, R.K., & Da Silva, J.R.P. 1999, *A&A*, 347, 550
- De Medeiros, J. R., do Nascimento, J. D., Jr., Sankarankutty, S., Costa, J. M., & Maia, M.R.G. 2000, *A&A*, 363, 239
- Denissenkov, P.A., & Weiss, A. 2000, *A&A*, 358, L49
- Drake, N.A. 1998, PhD Thesis - ON
- Eaton, J.A. 1995, *AJ*, 109, 1797
- Efremov, Yu.N., & Sitnik, T.G. 1988, *Sov. Astron. Lett.*, 14, 347
- Fekel, F.C. 1988, *A Decade of UV Astronomy with the IUE Satellite*, vol. 1, 331
- Fekel, F.C. & Marschall, L.A. 1991, *AJ*, 102, 1439
- Fekel, F.C., & Balachandran, S. 1993, *ApJ*, 403, 708
- Fekel, F.C., Webb, R.A., White, R.J., & Zuckerman, B. 1996, *ApJ*, 462, L95
- Fekel, F.C. 1997, *PASP*, 109, 514
- Fekel, F.C., & Watson, L.C. 1998, *AJ*, 116, 2466
- Gondoin, P. 1999, *A&A*, 352, 217
- Gregório-Hetem, J., Lépine, J.R.D., Quast, G.R., Torres, C.A.O., & de la Reza, R. 1992, *AJ*, 103, 549
- Gregório-Hetem, J., Castilho, B.V., & Barbuy, B. 1993, *A&A*, 268, L25
- Henry, G.W., Fekel, F.C., Hall, D.S. 1995, *AJ*, 110, 2926
- Henry, G.W., Fekel, F.C., Henry, S.M., & Hall, D.S. 2000, *ApJS*, 130, 201
- Hooten, J. T., & Hall, D. S. 1990, *ApJS*, 74, 225

- Houk, N., & Cowley, A.P. 1975, “Michigan Catalogue of two-dimensional spectral types for the HD stars”, Vol. 4., Ann Arbor: University of Michigan, Department of Astronomy
- Jasniewicz, G., Parthasarathy, M., de Laverny, P., & Thévenin, F. 1999, *A&A*, 342, 831
- Kjærgaard, P., Gustafsson, B., Walker, G.A.H., & Hultqvist, L. 1982, *A&A*, 115, 145
- Knauth, D. C., Federman, S. R., Lambert, D. L., & Crane, P. 2000, *Nature*, 405, 656
- Konstantinova-Antova, R., & Antov, A. 2000, Kinematics and Physics of Celestial Bodies. Suppl. Ser. N3, “Astronomy in Ukraine - 2000 and Beyond (Impact of International Cooperation)”, (ed. Ya.S. Yatskiv), p. 342
- Konstantinova-Antova, R.K., Antov, A.P., Bachev, R.S. 2000, *IVBS*, 4867, 1
- Kovacs, I. 1969, *Rotational Structure in the Spectra of Diatomic Molecules*, Akademiai Kiado, Budapest
- Kurucz, R.L. 1992, *Rev. Mex. Astron. Astrofis.*, 23, 45
- Kurucz, R. 1993, ATLAS9 Stellar Atmosphere Programs and 2 km s⁻¹ Grid, Smithsonian Astroph. Obs. CD-ROM no. 13
- Lambert, D.L. 1978, *MNRAS*, 182, 249
- Lambert, D.L., & Ries, L.M. 1981, *ApJ*, 248, 228
- Lindgård, A., & Nielsen, S.E. 1977, *At. Data Nucl. Data Tables*, 19, 533
- Lundström, I., Ardeberg, A., Maurice, E., & Lindgren, H. 1991, *A&AS*, 91, 199
- Mallik, S.V. 1993, *ApJ*, 402, 303
- McWilliam, A., & Rich, R.M. 1994, *ApJS*, 91, 749
- Mishenina, T.V., & Tsymbal, V.V. 1997, *Astron. Letters*, 23, 609
- Moore, C.E., Minnaert, M.G.J., & Houtgast, J. 1966, The Solar Spectrum from 2935 Å to 8770 Å, NBSM
- Pagel, B.E.J., Tautvaišiene, G., 1995, *MNRAS*, 276, 505
- Palacios, A., Charbonnel, C, Forestini, M. 2001, *A&A*, 375, 9
- Pavlenko, Ya.V., Savanov, I.S., Yakovina, L.A. 1999, *Astron. Rep.* 43, 671
- Percy, J.R., Wong, N., Bohme, D., et al. 1994, *PASP*, 106, 611
- Phillips, J. G., & Davis, S.P. 1968, *The Swan System of the C₂ Molecule*, University of California Press, Berkeley and Los Angeles

- Randich, S., Gratton, R., & Pallavicini, R. 1993, *A&A*, 273, 194
- Randich, S., Giampapa, M.S., & Pallavicini, R. 1994, *A&A*, 283, 893
- Reddy, B. E., Lambert, D.L., Hrivnak, B. J., & Bakker, E. J. 2002, *AJ*, in press
- Sackmann, I.-J., & Boothroyd, A.I. 1999, *ApJ*, 510, 217
- Sackmann, I.-J., & Boothroyd, A.I. 2000, in “The Light Elements and their Evolution” IAU Symp. 198, Natal - Brazil, p. 98
- Schmidt-Kaler, Th., 1982, in *Landolt-Börnstein: NS, Group VI*
- Siess, L., & Livio, M. 1999a, *MNRAS*, 304, 925
- Siess, L., & Livio, M. 1999b, *MNRAS*, 308, 1133
- Skinner, C.J., Sylvester, R.J., Graham, J.R., Barlow, M.J., Meixner, M., et al. 1995, *ApJ*, 444, 861
- Smith, G.H., & Shetrone, M.D. 2000, *PASP*, 112, 1320
- Snedden, C. 1973, *ApJ*, 184, 839
- Snedden, C., & Lambert, D. L. 1982, *ApJ*, 259, 381
- Strassmeier, K. G., & Hall, D.S. 1988, *ApJS*, 67, 453
- Strassmeier, K. G., Bartus, J., Cutispoto, G., & Rodono, M. 1997, *A&AS*, 125, 11
- Strassmeier, K., Washuettl, A., Granzer, Th., Scheck, M., & Weber, M. 2000, *A&AS*, 142, 275
- Tomkin, J., Luck, R.E., & Lambert, D.L. 1976, *ApJ*, 210, 694
- Torres, C.A.O., Quast, G., de la Reza, R., Gregório-Hetem, J., & Lépine, J.R.D. 1995, *AJ*, 109, 2146
- Torres, C.A.O. 1998, Internal Publication - ON
- Torres, C.A.O., Quast, G., de la Reza, R., & da Silva, L. 2000, in “The Light Elements and their Evolution” IAU Symp. 198, Natal - Brazil, p.320
- Torres, C.A.O., Quast, G., de la Reza, R., da Silva, L., Lépine, J.R.D., & Gregório-Hetem, J. 2002, to be submitted to the *AJ*
- Whitelock, P., Menzies, J., Feast, M., Catchpole, R., Marang, F., & Carter, B. 1995, *MNRAS*, 276, 219
- Wyller, A.A. 1966, *ApJ*, 143, 828

Fig. 1.— Star PDS 365. Top half: Iron abundances from Fe I lines *vs* equivalent width. Bottom half: Iron abundances from Fe I lines *vs* excitation potential.

Fig. 2.— Star PDS 365. The spectral region containing the Fe II line at 6084 Å. Observations are represented by separated points. The spectrum synthesis is made for the stellar parameters presented in Table 4.

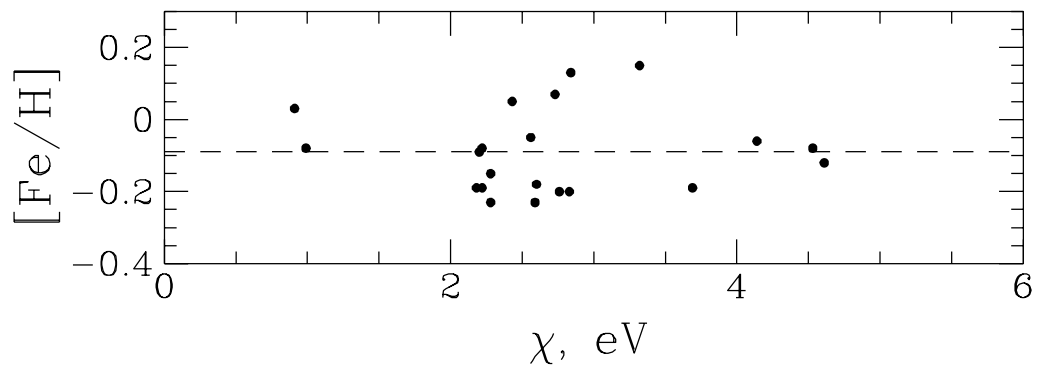
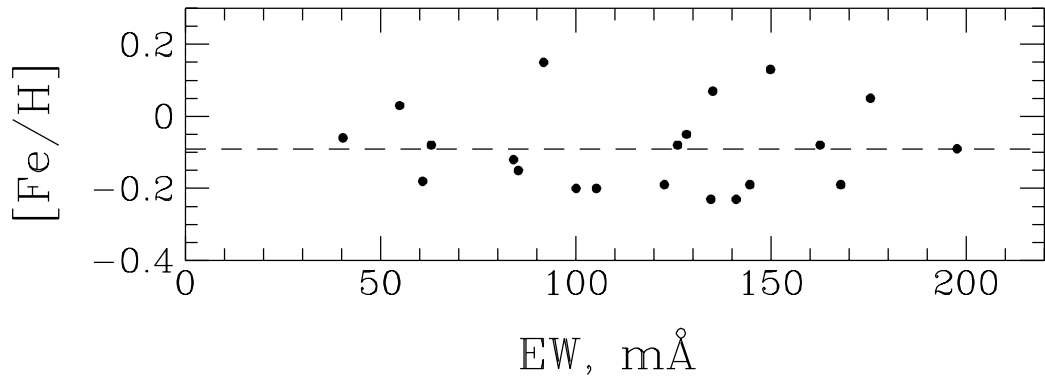
Fig. 3.— Star PDS 365. Observed (points) and synthetic (lines) spectra calculated with different values $^{12}\text{C}/^{13}\text{C} = 4, 8, 12, 20, \text{ and } 40$, $[\text{C}/\text{H}] = -0.1$, $[\text{N}/\text{H}] = 0.0$ and $[\text{O}/\text{H}] = -0.04$. The best fit is achieved with $^{12}\text{C}/^{13}\text{C} \sim 12$.

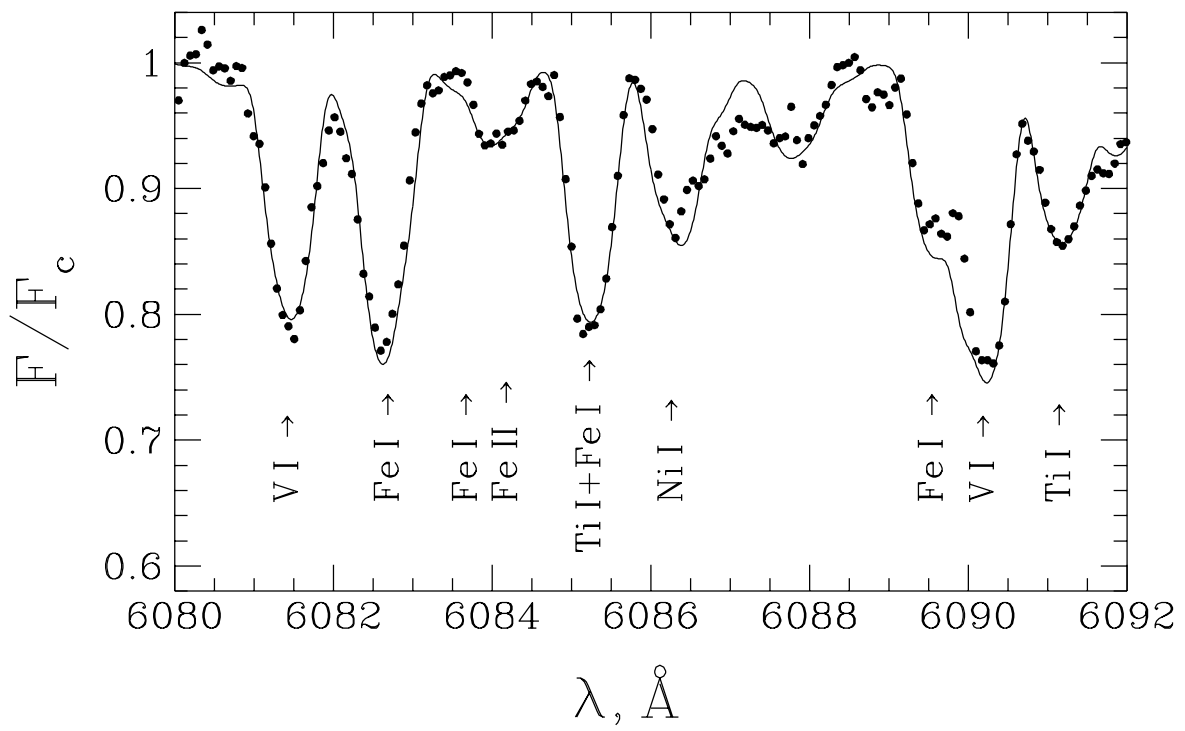
Fig. 4.— Star PDS 365. Calculations of the resonance Li I line corresponding to the total Li abundance $\log \varepsilon(\text{Li}) = 3.3$ for different $^6\text{Li}/^7\text{Li}$ ratios equal to 0.0, 0.05 and 0.10. The observed spectrum is best fitted with $^6\text{Li}/^7\text{Li} = 0.0$.

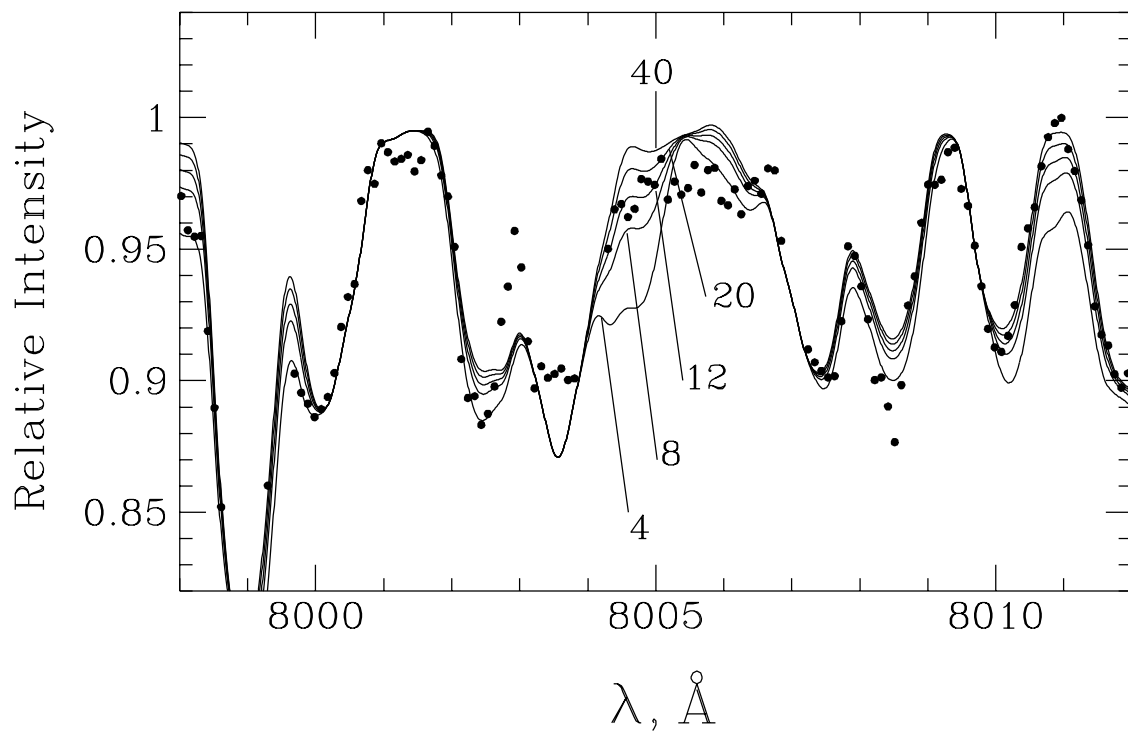
Fig. 5.— Star PDS 365. Spectra show the Li I features at 6708 Å and 6104 Å lines. Observed profiles are represented by separated points. Synthetic spectra are shown for four ^7Li abundances equal to 2.9, 3.1, 3.3 and 3.5. The best-fitting spectrum in both cases corresponds to the Li abundance $\log \varepsilon(\text{Li}) = 3.3$.

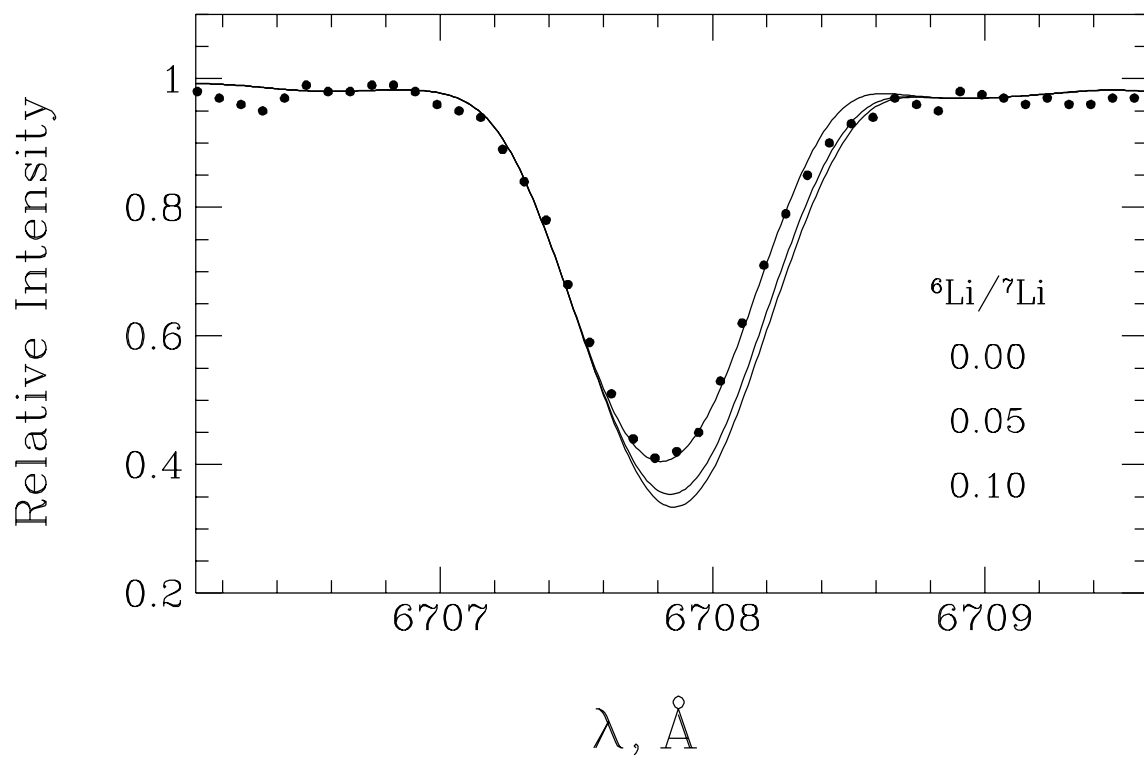
Fig. 6.— $\text{H}\alpha$ profiles of some representative giants. All spectra are presented on the same intensity scale, and corrected for stellar radial velocity. Vertical lines represent the heliocentric standard of rest. The $\text{H}\alpha$ profile for some stars have been obtained at different times spanning some years for PDS 365 and HD 219025 to a few days for HD 203251, HD 9746, HD 233517 and HD 219025.

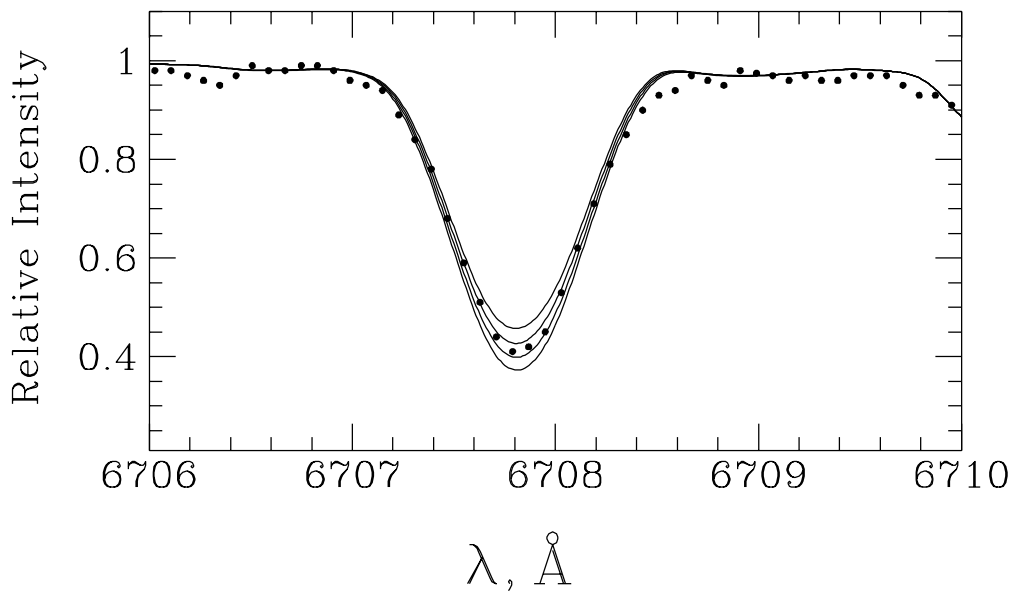
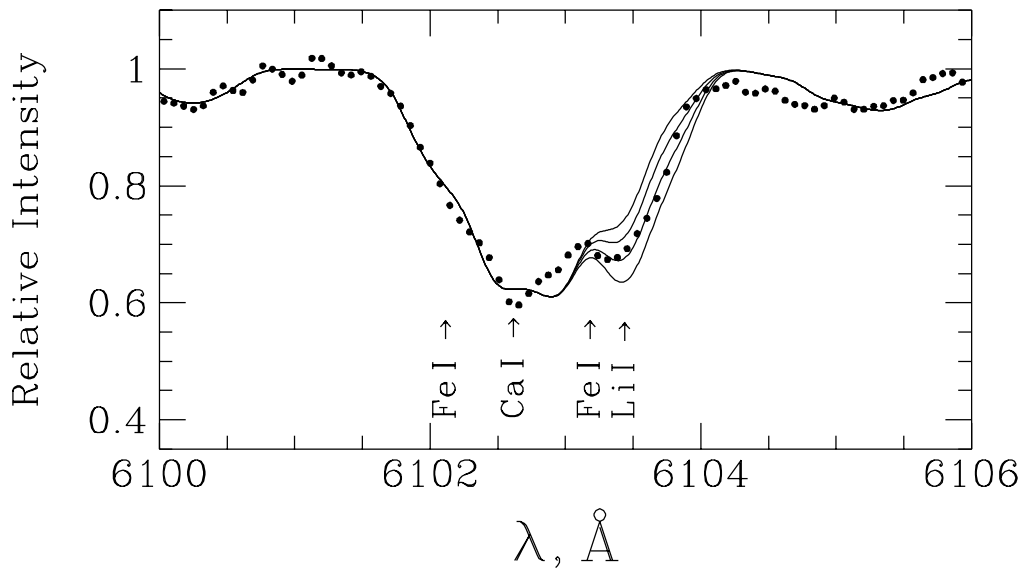
Fig. 7.— Distribution of the IRAS sources in a color-color diagram with flux densities at 12, 25 and 60 microns for rapidly-rotating giants (*a*) and for slowly-rotating giants (*b*). Filled symbols represent Li-rich objects. Triangles are IRAS sources with one or two flux limits. Open symbols correspond to Li-poor giants. Crosses – giants for which no observations in the Li line have been made.

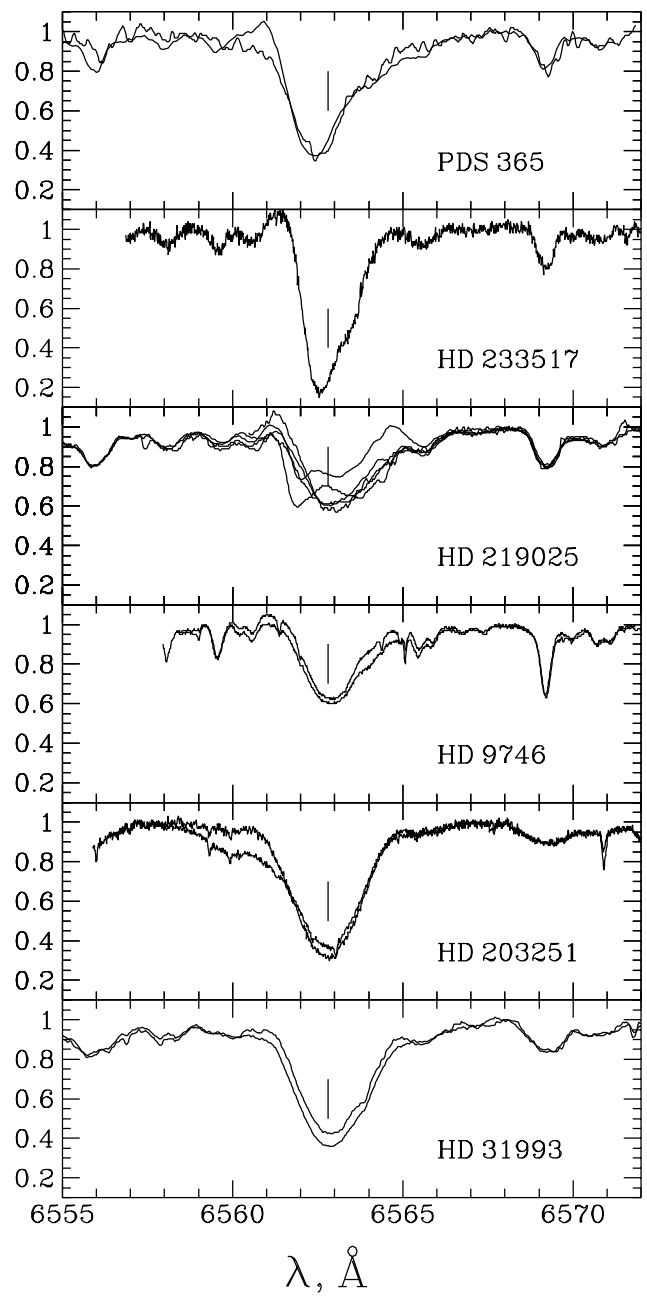


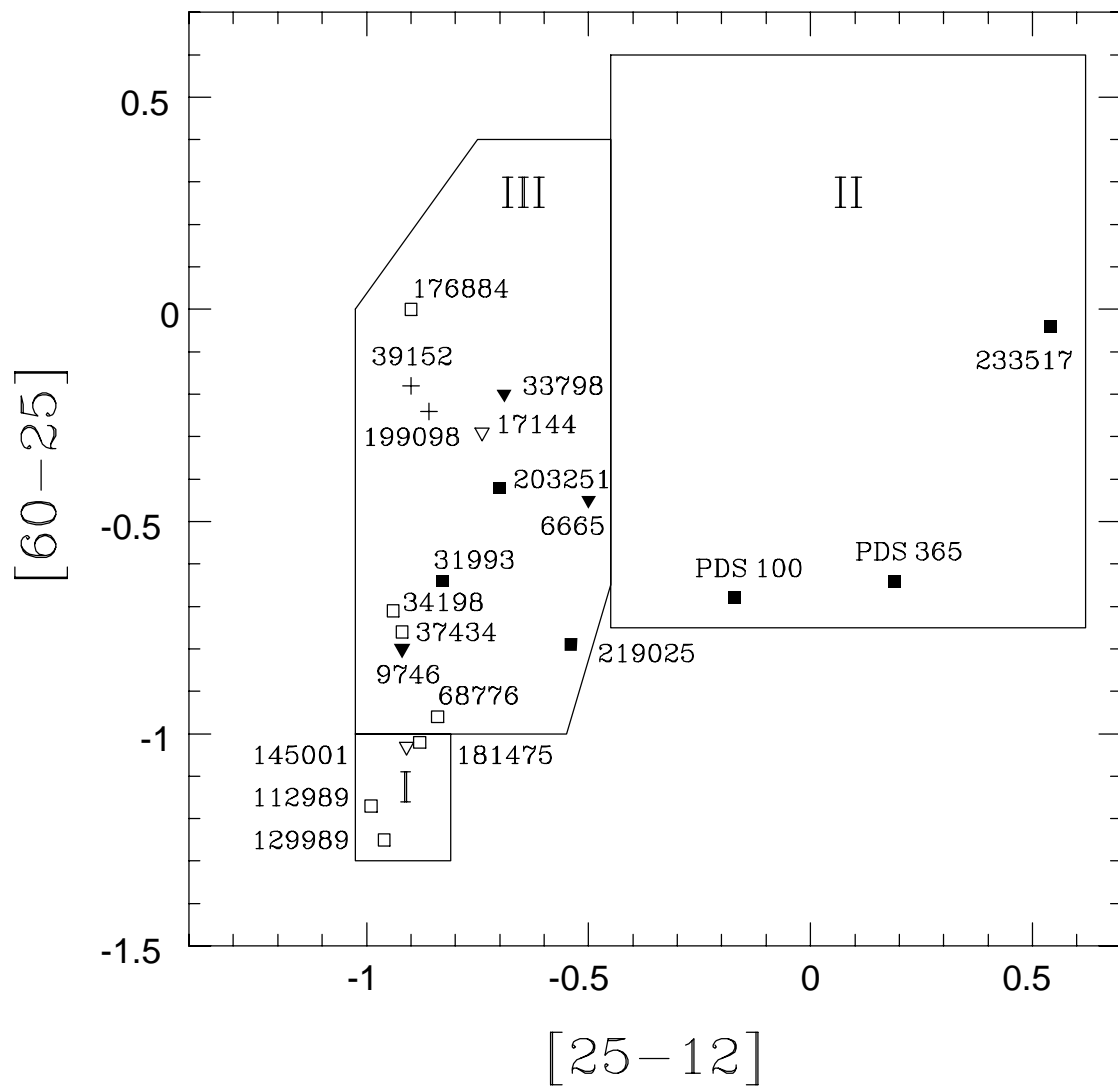












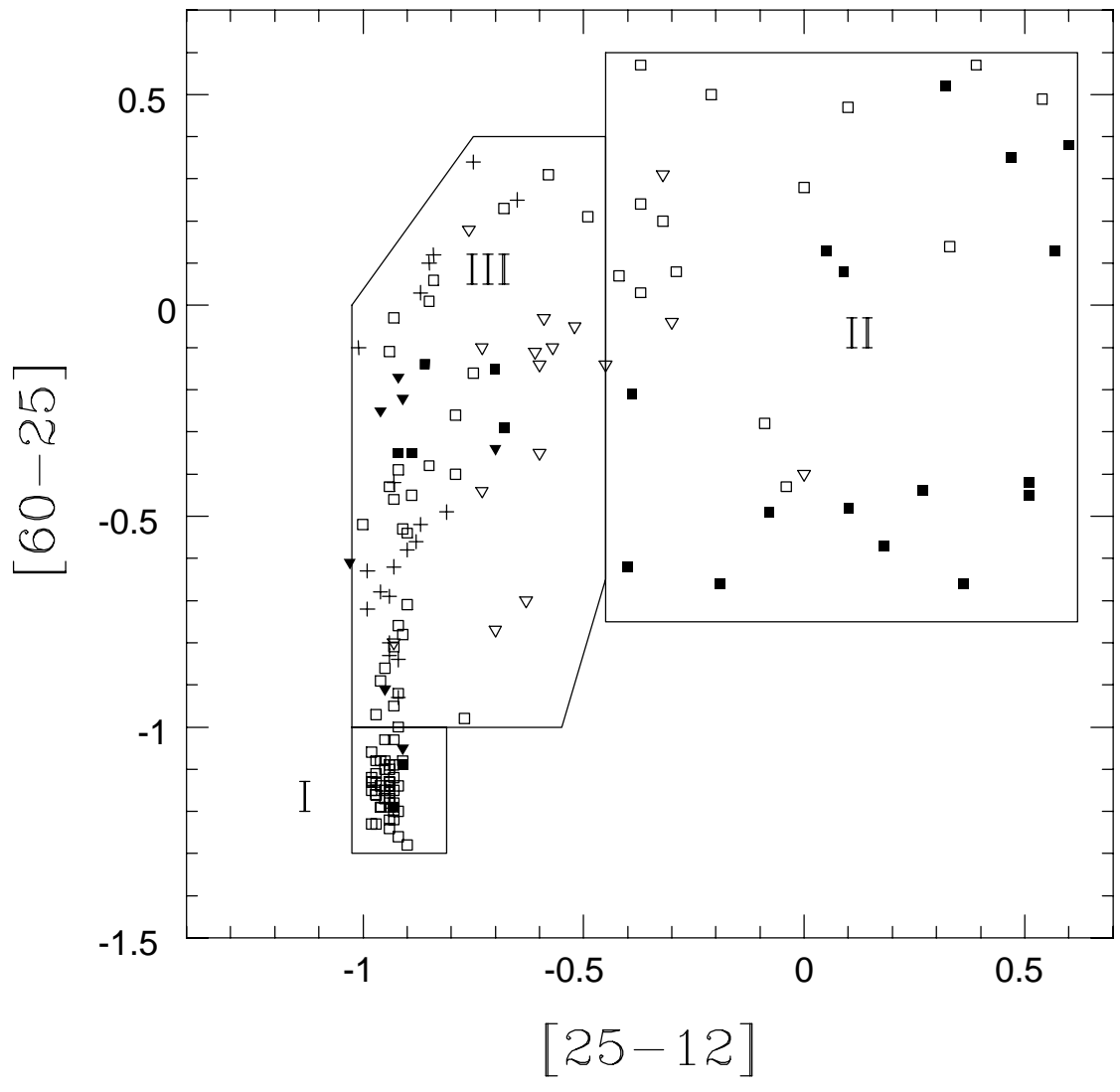


Table 1. Fast rotating giants, spectral types, magnitudes, rotation velocities, Li abundances and manifestations of activity

Star	Sp. Type	V	$v \sin i$ (km s ⁻¹)	EW(Li) (mÅ)	log ϵ (Li)	Activity
BD+25 4819	K0 II	10.94	14.9 ¹⁰	< 10 ¹⁹		
BD+31 2471	K0 II	10.9	13.8 ¹⁰			
BD+70 959	K0 III	9.64	23 ⁷	90 ⁷	1.8 ²	X-ray, Ca II
HD 6665	G5 III	8.44	10 ¹⁴ , 7.9 ¹⁴ , 6.0 ¹⁹	398 ¹⁴ , 405 ¹⁹	2.92 ¹⁴ , 2.7 ¹⁹	Ca II
HD 9746	K1 III	6.22	8 ² , 8.7 ¹⁰	396 ² , 455 ¹³ , 518 ¹⁹	2.8 ² , 3.6 ¹² , 3.75 ¹³ , 3.5 ¹⁹	X-ray, flares, Ca II
HD 17144	K1 III/G8 III-IV	8.27	15 ² , 18.9 ¹⁰	55 ² , 85 ¹⁹	1.1 ² , 0.85 ³	X-ray, Ca II
HD 31993	K2 III	7.49	33.4 ⁵ , 31.1 ¹⁰	144 ² , 174 ¹⁹	1.4 ² , 1.0 ³ , 1.7 ¹⁶	X-ray, Ca II
HD 33798	G8 III	6.92	33.1 ⁵	46 ²	1.5 ² , 1.8 ¹	X-ray, flares, Ca II
HD 34198	K0 III	6.95	15 ² , 18.7 ¹⁰	13 ²	0.4 ² , < -0.2 ³	Ca II
HD 37434	K2 III	6.10	46 ² , 65 ¹⁰		< -0.15 ³	X-ray, Ca II
HD 39152	K0 II	7.41	8.0 ¹⁰			
HD 68776	G8 III	6.37	8.9 ¹⁰		1.1 ¹⁹	
HD 112989	G9 III CH-2F	4.90	11.0 ¹⁰ , 12 ¹⁵		+0.9 ¹	X-ray, flares, Ca II
HD 129989	K0 II-III	2.70	8.4 ¹⁰	< 10 ¹⁹		
HD 145001	G8 III	5.00	9.9 ¹⁰		< +0.5 ¹	X-ray
HD 176884	K0 III	6.01	15.0 ¹¹		1.2 ¹¹	
HD 181475	K5 II, K7 IIa	6.96	8.2 ⁵ , 8.4 ¹⁰	< 10 ¹⁹		Ca II
HD 185958	G8 IIIa CN 0.5	4.39	9.9 ¹⁰		< 0.3 ¹ , 0.2 ⁶	
HD 199098	K0 II	5.47	10.7 ¹⁰			
HD 203251	K2 III	8.03	40 ² , 44.8 ¹⁰	214 ¹⁹	1.4 ² , 1.5 ¹⁹	Ca II
HD 219025	K2 III	7.68	20 ³ , 23 ¹¹	456 ⁹ , 428 ¹⁹	3.3 ⁹ , 3.0 ¹¹ , 2.9 ¹⁹	Ca II
HD 232862	G8 II	9.46	20.6 ¹⁰			X-ray
HD 233517	K2 III/II	9.4	17.6 ¹³	550 ⁸ , 546 ¹³	3.9 ⁸ , 4.22 ¹³	Ca II
HD 284857	K2 II	9.30	8.0 ¹⁰ , 4.5 ¹⁹	43 ¹⁹	0.3 ¹⁹	
PDS 100	K0-2 III	10.45	9 ¹⁷	372 ¹⁷	2.5 ¹⁷	Ca II
PDS 365	K1 III	13.15	20 ¹⁹	450 ¹⁹ , 465 ¹⁸	3.3 ¹⁹	Ca II

References. — ¹Brown et al. 1989, ²Fekel & Balachandran 1993, ³Randich et al. 1993, ⁴Fekel et al. 1996, ⁵Fekel 1997, ⁶Mishenina & Tsymbal 1997, ⁷Ambruster et al. 1997, ⁸Drake 1998, ⁹Fekel & Watson 1998, ¹⁰de Medeiros & Mayor 1999, ¹¹Jasniewicz et al. 1999, ¹²Pavlenko et al. 1999, ¹³Balachandran et al. 2000, ¹⁴Strassmeier et al. 2000, ¹⁵Henry et al. 2000, ¹⁶Castilho et al. 2000, ¹⁷Reddy et al. 2002, ¹⁸Torres et al. 2002, ¹⁹This work.

Note. — Lithium abundances in references 12 and 13 are in non-LTE.

Table 2.

Star	Telescope	Spectrograph	Spectral Region	Date
PDS 365	CTIO, 4.0m	Coude	5120 Å – 8370 Å	05/01/96
PDS 365	ESO, 1.52m	FEROS	3800 Å – 9000 Å	06/05/01
BD+25 4819	ESO, 1.52m	FEROS	3800 Å – 9000 Å	09/09/01
HD 6665	ESO, 1.52m	FEROS	3800 Å – 9000 Å	12/10/00
HD 9746	McDonald, 2.7m	Coude	5680 Å – 8150 Å, with gaps	11/05/97 11/09/97
HD 17144	ESO, 1.52m	FEROS	3800 Å – 9000 Å	12/05/00
HD 31993	ESO, 1.52m	FEROS	3800 Å – 9000 Å	12/05/00 12/07/00 12/09/00
HD 68776	ESO, 1.52m	FEROS	3800 Å – 9000 Å	12/06/00
HD 129989	ESO, 1.52m	FEROS	3800 Å – 9000 Å	06/02/01
HD 181475	ESO, 1.52m	FEROS	3800 Å – 9000 Å	06/02/01
HD 203251	McDonald, 2.7m	Coude	5680 Å – 8150 Å, with gaps	11/05/97 11/09/97
HD 233517	McDonald, 2.7m	Coude	5680 Å – 8150 Å, with gaps	11/06/97 11/08/97
HD 219025	ESO, 1.40m	CAT CES Multichannel	5890 Å, 6700 Å	09/18/98
	ESO, 1.52m	FEROS	3800 Å – 9000 Å	22/06/99 12/23/99 07/23/00 08/21/00 10/08/00 12/14/00 12/15/00 12/16/00 01/31/01
HD 284857	ESO, 1.52m	FEROS	3800 Å – 9000 Å	12/05/00
ϵ Vir	ESO, 1.52m	FEROS	3800 Å – 9000 Å	08/12/01

Table 3.

Ion	$\lambda, \text{\AA}$	$\chi,$ eV	$\log gf$	EW_{obs} m \AA	[Fe/H]
Fe I	6151.623	2.18	−3.33	122.7	−0.19
	6173.341	2.22	−2.86	144.6	−0.19
	6180.209	2.73	−2.65	135.1	0.07
	6229.232	2.83	−2.82	105.3	−0.20
	6271.283	3.32	−2.80	91.8	0.15
	6297.799	2.22	−2.66	162.6	−0.08
	6322.694	2.59	−2.43	141.1	−0.23
	6335.337	2.20	−2.17	197.7	−0.09
	6336.830	3.69	−0.66	167.9	−0.19
	6353.849	0.91	−6.36	54.9	0.03
	6355.035	2.84	−2.32	149.9	0.13
	6392.538	2.28	−3.95	85.3	−0.15
	6475.632	2.56	−2.92	128.4	−0.05
	6481.878	2.28	−2.98	134.6	−0.23
	6574.254	0.99	−5.00	126.1	−0.08
	6593.874	2.43	−2.37	175.5	0.05
	6627.560	4.53	−1.55	63.0	−0.08
6646.966	2.60	−3.91	60.8	−0.18	
6653.911	4.14	−2.44	40.4	−0.06	
6703.576	2.76	−3.05	100.1	−0.20	
6705.105	4.61	−1.06	84.1	−0.12	
Fe II	6416.928	3.89	−2.68	47.5	−0.13
	6432.683	2.89	−3.55	66.9	−0.06
	6456.391	3.90	−2.28	68.1	−0.08

Table 4. Main parameters of PDS 365

Parameter	Value	Parameter	Value	Parameter	Value
T_{eff}	4540 ± 150 K	$(B - V)_{\text{obs}}$	1.50^{m}	[Fe/H]	-0.09 ± 0.05
$\log g$	2.20 ± 0.3	d	1.6 kpc	[C/H]	-0.1
ξ_{m}	1.8 ± 0.2 km s $^{-1}$	V_{rad}	-38.3 ± 0.5 km s $^{-1}$	[N/H]	0.0
L	$72L_{\odot}$	$v \sin i$	20.0 ± 1.0 km s $^{-1}$	[O/H]	-0.04
M	$1.1M_{\odot}$			$^{12}\text{C}/^{13}\text{C}$	12_{-8}^{+2}
R	$14R_{\odot}$			$\log \varepsilon(\text{Li})$	3.3 ± 0.2

Note. — Due to the absence of Hipparcos parallax measurements of PDS 365, L , M , R and d have only approximate values. This is also the case of [O/H] due to the presence of night sky emission at the [O I] 6300 Å line.

Table 5. Comparative CNO abundances

Star	[C/Fe]	[N/Fe]	[O/Fe]	[Fe/H]	$^{12}\text{C}/^{13}\text{C}$	$(T_{\text{eff}}, \log g)$
PDS 365 ⁵	−0.01	+0.09	+0.05	−0.09	12	(4540, 2.2)
PDS 100 ¹	−0.07	+0.06	−0.05	+0.14	9	(4500, 2.5)
HD 9746 ²	−0.08	−0.16	−0.05	−0.13	24	(4420, 2.3)
ϵ Vir ⁵	−0.25	+0.19	−0.35	+0.05 ^a	20	(5000, 2.5)
ϵ Vir ³	−0.35	+0.09	−0.28	+0.05	20 ⁴	(5060, 2.7)

References. — ¹Reddy et al. 2002, ²Berdyugina & Savanov (1994),
³Kjærgaard et al. (1982), ⁴Lambert & Ries (1981), ⁵This work.

Note. — The solar abundances used in (2) and (5) are $\log \varepsilon(\text{C}_{\odot}) = 8.56$,
 $\log \varepsilon(\text{N}_{\odot}) = 8.05$, $\log \varepsilon(\text{O}_{\odot}) = 8.93$, and $\log \varepsilon(\text{Fe}_{\odot}) = 7.50$.

Note. — ^a[Fe/H] adopted from (3)